Performance analysis of a radial flux PM machine using a hybrid analytical model and a MBG reluctance network model

Abdourahman Aden Diriyé[1], Yacine Amara[1], Georges Barakat[1], Sami Hlioui[2], Olivier De La Barrière[2], Mohamed Gabsi[2]

1. GREAH, EA3220, Université du Havre
  75 rue Bellot, 76058 Le Havre, France

  prenom.nom@univ-lehavre.fr

2. SATIE, UMR CNRS 8029
  61 av. du Président Wilson, 94235 Cachan, France

  prenom.nom@satie.ens-cachan.fr

ABSTRACT. In this contribution, open circuit performances (flux linkage, EMF, cogging torque, open-circuit iron loss) of a permanent magnet radial flux rotating machine are analysed using a new hybrid analytical model and a mesh-based generated reluctance network model (MBGRN). The hybrid analytical model (HAM) is based on strong coupling of analytical solution of Maxwell's equations with reluctance network (RN). It is shown that the hybrid analytical model allows to combine advantages of analytical and reluctance networks modeling approaches. As compared to reluctance networks modeling, the new approach helps reduce calculation time while giving fairly good results.

RÉSUMÉ. Les performances à vide d'une machine rotative à flux radial à aimants permanents sont étudiées dans cet article grâce à deux approches de modélisation relativement nouvelles : un modèle analytique hybride (HAM) et un circuit de réluctances généré à partir du maillage du domaine d'étude (MBGRN). Le modèle hybride est basé sur le couplage direct de la solution analytique des équations de Maxwell dans l'entrefer magnétique et un circuit de réluctances (RN). Il est montré que le modèle hybride permet de réduire le temps de calcul en comparaison de l'approche circuits de réluctances.

KEYWORDS: Maxwell equations, analytic modeling, reluctance networks, magnetic equivalent circuits, direct coupling, air-gap modeling.

MOTS-CLÉS : équations de Maxwell, modélisation analytique, réseaux de perméances, cicruits magnétiques équivalents, couplage direct, modélisation de l'entrefer.

1. Introduction

Finite-Element (FE) method is used since a long time for the design and analysis of electromagnetic devices. However, FE analysis is high time consuming, especially at firsts design stages. In order to reduce pre-design stages duration, engineers working in R&D departments often prefer the use of analytical models. Two types of models are often used: magnetic equivalent circuits (MEC), also known as reluctance networks (RN), and analytical models (Tiegna *et al.,* 2013) based on the formal solution of Maxwell's equations in constant permeability regions. However, as compared to FE method, MEC or RN are not as generic. Classical RN models have to be adapted if the geometry structure is varying, and even in the case of a given structure geometry, the RN has to be adapted if the geometric parameters vary in a large scale. Furthermore, the air-gap modeling for RN method is often an issue. To remedy to this problem of genericity some authors have proposed a new MEC (RN) method (Nedjar, 2011; Sykulski, 1995; Perho, 2002; Amrhein, Krein, 2009; Mirzaei *et al.,* 2007) to compete with the finite element method. In this approach, the RN is generated from a mesh of the studied domain. However, in contrast to FE method, it should be noticed that till now commercial software packages based on this method still not available. Analytical models based on the formal solution of Maxwell's equations help overcome aforementioned problem, but neglect magnetic saturation.

In order to combine advantages of both methods, genericity, reduced computation time, air-gap modeling and magnetic saturation consideration, a new modeling approach, based on the direct (strong) coupling of analytical solution of Maxwell's equations and mesh-based generated reluctance networks, is used in this study (Gholizad *et al.*, 2006; Mirzaei *et al.,* 2007). While the approach used by the authors in (Gholizad *et al.*, 2006; Mirzaei *et al.,* 2007) is based on the magnetic vector potential analytical solution, the approach adopted in this paper is based on the analytical solution of the magnetic scalar potential in low permeability regions (permanent magnet and air-gap regions). The MBGRN method is used to model the stator (Nedjar, 2011; Sykulski, 1995; Perho, 2002; Amrhein et Krein, 2009; Mirzaei *et al.,* 2007).

In (Ouagued *et al.,* 2014), the authors used a similar approaches (HAM and MBGRN) to study open circuit performances of a linear structure. In this paper the same approaches are applied to study open circuit performances (flux linkage, EMF, cogging torque, open-circuit iron loss) of a surface mounted radial field rotating machine. It is shown that both approaches are as accurate as FE analysis, the HAM being faster as compared to MBGRN. The goal of this study is to show that these approaches can be applied to different structures. These approaches are complementary to FE method.

2. Radial field PM rotating machine

Figure 1 shows the structure which has been modeled using the three methods: FE, RN (reluctance networks) model, and HAM. It is a radial field surface mounted PM rotating machine, with classical distributed windings. The dimensions of the machine have been chosen to simplify the modeling study.

Table 1 gives main machine's characteristics. This figure also shows how the HAM model is structured. The mobile armature is considered having an infinite relative permeability to simplify the modeling study.

Table 1. Machine' parametres

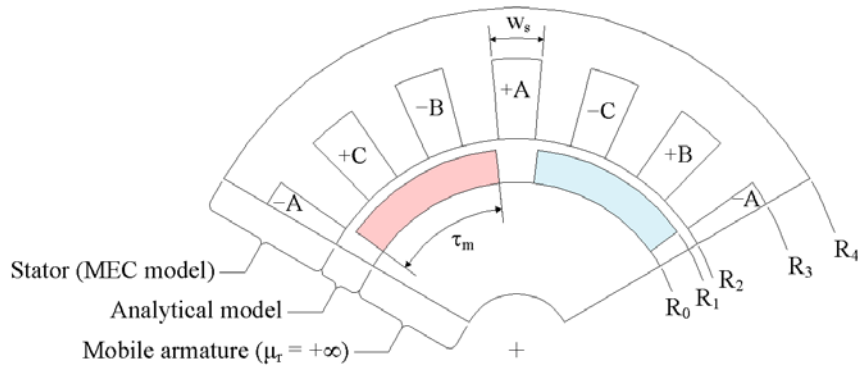|	
Mechanical air-gap e (mm)	1
Number of pole pairs	3
Pole pitch τ_p (rad)	$\pi/3$
R_0, R_1, R_2, R_3 and R_4 (mm)	50, 60, 61, 81, 91
τ_m (rad)	$0.9 \cdot \tau_p$
w_s (rad)	$\pi/18$
Magnetisation type	Radial magnetisation
PM magnetic remanence (T)	1.2

Figure 1. Cross section view of the studied machine

2.1. Finite element modeling

The studied structure has been first modeled using finite element method. Results obtained from this method will be considered as the reference to which the quality of results obtained from the two other methods will be assessed. Open circuit performances are compared.

Figure 2 shows the different boundary conditions applied in order to perform the FE analysis. Roughly same conditions are applied for the two other approaches. Instead of cyclic boundary conditions, anti-periodic boundary conditions are used. The goal of this paper being to compare RN modeling and HAM essentially in term of computation time, the magnetic saturation has not been considered. Thus, stator core is assumed to have a constant relative permeability of 7500.

A second order FE method is used to solve the 2D magnetostatic field formulation in term of vector potential. Local and global quantities can then be derived from FE simulations for the comparison study.
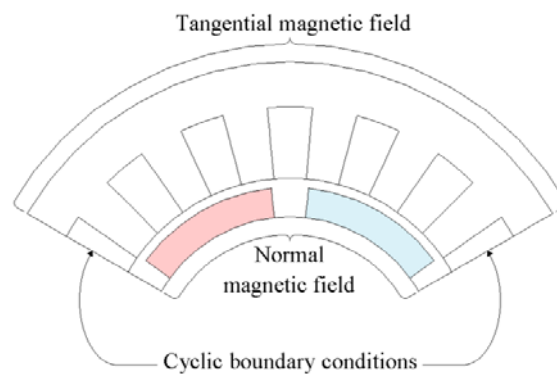

Figure 2. Boundary conditions for the FE model

3. Reluctance network model

Reluctance network method, based on a mesh, has been used for the modeling of the studied structure. Although this approach is relatively old (Nedjar, 2011 ; Sykulski, 1995 ; Perho, 2002 ; Amrhein et Krein, 2009 ; Mirzaei *et al.,* 2007) and gives relatively good results, as will be seen, it is still not widely spread. As finite element method, this approach consists of meshing the studied domain. Reluctance elements are used for the mesh. Figure 3 shows reluctance elements which can be used for 2D problems. Regarding the studied machine structure, 2D quadrilateral reluctance elements (Figure 3a) have been used.
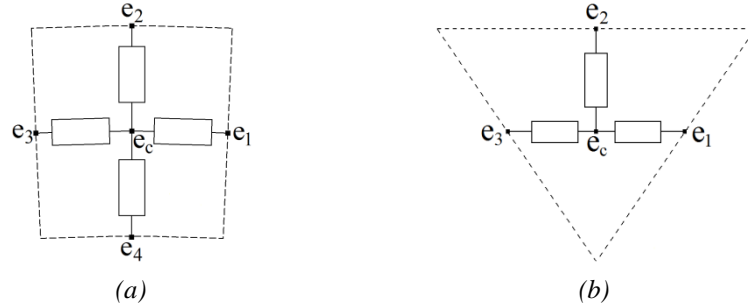
(a)   *(b)*

Figure 3. Reluctance elements for 2D problems

Figure 4 illustrates this modeling approach. In order to have a normal magnetic field boundary condition between the translator iron core and the permanent magnet region, a constant value of the magnetic scalar potential is imposed. It is set equal to 0 A.m (lower part of Figure 4). Air outside the stator core is not considered and a tangential magnetic flux is imposed at the air-stator frontier (radial direction). At both circumferential ends (circumferential direction) anti-periodic boundary conditions are imposed.

In order to compute the cogging toque with a relatively good precision, two layers of elements are imposed in the air-gap in radial direction. The number of elements in circumferential direction is chosen equal to 120, and 82 in radial direction. It is then possible to use reluctance elements as the one shown in Figure 3a to mesh the studied domain. The number of nodes is then equal to nn = 9840.

The nodal method is used for formulating the RN equations system. The unknowns for the generated circuit equations system are the magnetic scalar potentials at each node. Figure 5 illustrates how the equations corresponding to a given node are determined from Kirchhoffs's laws.

The RN method results in a set of linear Equation (1) which should be solved to obtain magnetic scalar potentials.

$$[P] \cdot [U] = [\Phi] \tag{1}$$

[P] (nn × nn) is the permeances matrix; [Φ] (nn × 1) is the source vector, elements of which are related to geometry distribution and physical properties of magnetic field sources (magnetic remanence and current density distributions) and [U] (nn × 1) is the unknowns vector (the magnetic scalar potentials in each node).
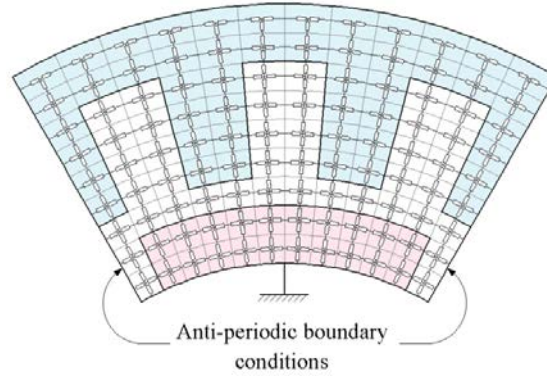
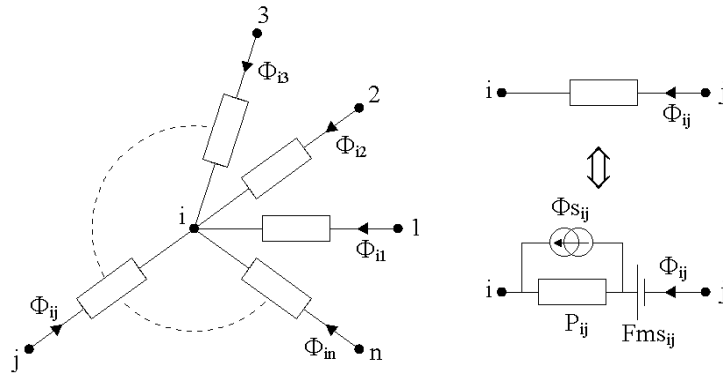*Figure 4. Illustration of the RN modeling based on the mesh of the studied domain*

Figure 5. Equation setting for the ith node

According to Kirchoff's laws, it can be established that

$$\begin{cases} \displaystyle\sum_{\substack{j=1 \\ j \neq i}}^{n} \Phi_{ij} = 0 \, Wb \\[2mm] U_i - U_j = Fms_{ij} - \dfrac{(\Phi_{ij} - \Phi s_{ij})}{P_{ij}} \end{cases} \quad (2)$$

and then,

$$\left(\sum_{\substack{j=1 \\ j\neq i}}^{n} P_{ij} \right) U_i + \sum_{\substack{j=1 \\ j\neq i}}^{n} (-P_{ij}) U_j = \sum_{\substack{j=1 \\ j\neq i}}^{n} (\varPhi s_{ij} + P_{ij} Fms_{ij}) \tag{3}$$

The motion is then taken into account by simply modifying the source vector [Φ]. The minimum displacement step is equal to the angular distance between two adjacent nodes in circumferential direction. In our case the machine has been meshed uniformly with 120 elements in circumferential direction and 82 in radial direction, which means that the angular distance between two adjacent nodes in circumferential direction is equal to 0.5°.

Apart from permanent magnet region, all reluctance elements branches are constituted of passive permeances. Permanent magnets can either be modeled by a flux source in parallel with a permeance or a magnetomotive force MMF in series with a permeance, as shown in Figure 6.
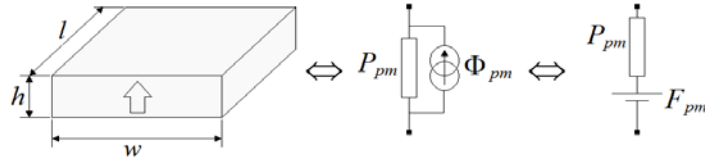

Figure 6. A permanent magnet region modeling

Expressions of the different parameters of a permanent magnet region model depend on PM characteristics and the region geometry and dimensions. These expressions for a parallelogram PM region are given by

$$\begin{cases} P_{pm} = \mu_0 \mu_r \dfrac{lw}{h} \\[2mm] \varPhi_{pm} = B_r lw \\[2mm] F_{pm} = \dfrac{B_r}{\mu_0 \mu_r} h \end{cases} \tag{4}$$

4. Hybrid analytical model

The new hybrid analytical model is based on a strong coupling between the MEC method and analytical models based on the formal solution of Maxwell's equations. This coupling can help solve the problem of air-gap modeling in MEC method, and

the consideration of the local magnetic saturation in modeling approaches involving analytical technique.

Figure 1 illustrates how the two approaches are combined. The analytical solution is used for modeling the magnetic air-gap region (PM and mechanical air-gap regions). The MBGRN method is used to model the stator part (slots and stator iron core). The direct coupling of both methods is presented in following sections.

4.1. Analytical model

The magnetic scalar potential U in regions I (PM region, $r \in [R_0, R_1]$) and II (air-gap region, $r \in [R_1, R_2]$) is governed by the following partial differential equations:

$$
\begin{cases}
\dfrac{\partial^2 U}{\partial r^2} + \dfrac{1}{r^2}\dfrac{\partial^2 U}{\partial \varphi^2} + \dfrac{1}{r}\dfrac{\partial U}{\partial r} = \dfrac{B_{rr}}{\mu_0 \cdot r}, & \text{for region I} \\[3mm]
\dfrac{\partial^2 U}{\partial r^2} + \dfrac{1}{r^2}\dfrac{\partial^2 U}{\partial \varphi^2} + \dfrac{1}{r}\dfrac{\partial U}{\partial r} = 0, & \text{for region II}
\end{cases}
\tag{5}
$$

where B_{rr} is the radial component of the PM remanent flux density. The PM permeability is assumed to be equal to that of air.

By combining the general solution of these equations, with boundary conditions at $r = R_0$ and $r = R_1$, the solution of the magnetic scalar potential in air-gap region is given by equation (6).

$$
U^{II} = \sum_{n=1}^{+\infty}
\begin{bmatrix}
\left(b_{1n} \cdot r^{p \cdot n} + b_{2n} \cdot r^{-p \cdot n} \right) \cdot cos(\, p \cdot n \cdot \varphi \,) \\
+ \\
\left(b_{3n} \cdot r^{p \cdot n} + b_{4n} \cdot r^{-p \cdot n} \right) \cdot sin(\, p \cdot n \cdot \varphi \,)
\end{bmatrix}
\tag{6}
$$

where p is the number of pole pairs. b_{1n}, b_{2n}, b_{3n} and b_{4n} are the unknowns. In PM region (region I), the coefficients of magnetic scalar potential depend on the coefficients B_{rn} of Fourier series representation of the PM remanent flux density (7).

$$
B_{rr} = \sum_{n=1}^{+\infty} B_{rn} \cdot \sin\left(n \cdot p \cdot \varphi_r \right)
\tag{7}
$$

where φ_r is the circumferential space coordinate in the rotor referential.

4.2. Mesh based generated RN modeling of stator

In order to have a more generic approach, the stator is modeled using reluctance network technique based on the mesh of studied domain (Nedjar, 2011; Sykulski,

1995; Perho, 2002; Amrhein et Krein, 2009; Mirzaei *et al.,* 2007). This technique can be used with a minimum number of reluctances for regions where flux tubes are not highly affected by topology changes whether it is due to motion or to geometric dimensions variations.

In order to have a like for like comparison, the stator is meshed in the same way as the RN model presented in section 3. The stator is meshed with 7200 quadrilateral elements, 120 elements in circumferential direction and 60 in radial direction.

4.3. Direct coupling method

Figure 7 illustrates the coupling between both approaches (AM and RN). The coupling between both models is obtained by equalizing magnetic scalar potentials at $r = R_2$, and computing the incoming fluxes at nodes located at $r = R_2$, using the radial component of air-gap flux density vector obtained from the analytical solution.

$$U^{II}(r = R_2, \varphi) = U^{RN}(\varphi) \tag{8}$$

$$P_{ij}(U_i - U_j) = -\mu_0\, l_a \int_{\varphi_{i1}}^{\varphi_{i2}} \left.\frac{\partial U^{II}}{\partial r}\right|_{r=R_2} d\varphi \tag{9}$$

where, U^{II} and U^{RN} refer to the scalar magnetic potentials obtained from the AM model (in the air-gap) and Fourier series expression obtained from discrete values of magnetic scalar potential of nodes located at the interface, respectively. R_2 is the r coordinate of the interface between both models. l_a is the machine's active length. P_{ij}, U_i and U_j are the permeance between nodes i and j, and magnetic scalar potential values at nodes i and j respectively (Figure 7).

The strong coupling results in a set of linear Equations (10) which should be solved to obtain the Fourier series coefficients of the scalar magnetic potential related to the formal analytical solution, and the magnetic scalar potential values at the nodes of the RN.

$$[A] \cdot [X] = [B] \tag{10}$$

$[A]$ $[(2 \cdot N_H + nns) \times (2 \cdot N_H + nns)]$ contains elements from the analytical solution and permeances from the RN model. $[B]$ $[(2 \cdot N_H + nns) \times 1]$ is the source vector, elements of which are related to geometry distribution and physical properties of magnetic field sources (magnetic remanence and current density distributions) and $[X]$ $[(2 \cdot N_H + nns) \times 1]$ is the unknowns vector. N_H is the number of harmonic considered in the analytical solution ($N_H = 70$) and nns is the number of nodes of the RN used to model the stator part (nns = 7320).

The rotor motion can be taken into account by replacing φ_r in Equation (7) by

$$\varphi_r = \varphi - \varphi_d \tag{11}$$

where, φ_d is the displacement angle. The motion will induce a change in $[B]$ vector. Figure 8 shows the flow chart of main steps of HAM modeling approach. This flow chart is similar to the other modeling approaches.
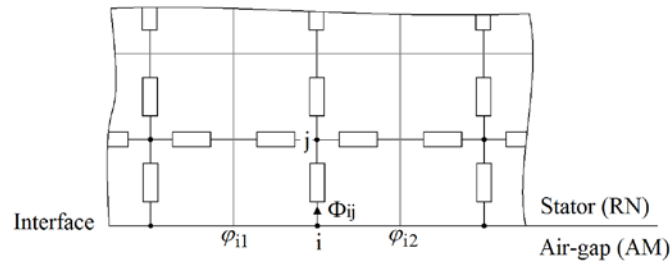

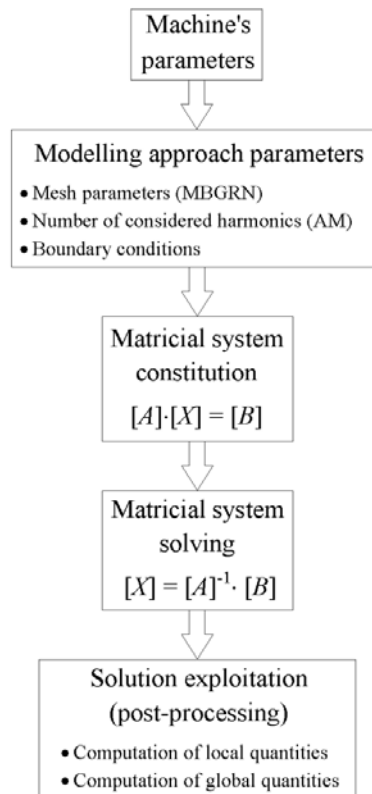*Figure 7. Illustration of the direct coupling at models interface*

Figure 8. Flow chart of HAM modelling approach

5. Calculation of global quantities

Calculation of global quantities allows evaluating open circuit machines performance. Furthermore, global quantities can be used for the coupling of developed model with electric circuit equations. It can then be used to study behavior of electric machines when connected to power converters and so for sizing and optimization purposes.

5.1. Computation of magnetic flux and EMF

The computation of the magnetic flux linking a coil is at the base of the calculation of EMF, and self and mutual inductances. For the studied machine, the phase flux linkage is computed by summing fluxes in the RN branches located at $r = (R_2 + R_3)/2$, at mid-height of the slots, and spanning one pole pitch, which corresponds to the opening distance of a phase coil for the studied machine.

The open-circuit flux linkage, and the EMF, are computed by only considering the PM as the field source (null armature currents). The EMF is calculated by differentiating the open-circuit flux linkage. The self and mutual inductances are computed by removing the PM and imposing the current in one phase.

5.2. Computation of cogging torque

Maxwell stress tensor (MST) method has been used for the computation of cogging torque for both modeling approaches. The Maxwell stress tensor method is applied to a surface located in the air-gap at the PM surface ($r = R_1$) for the AM:

$$\Gamma_{cogging} = \frac{l_a \cdot p \cdot R_1^{\,2}}{\mu_0} \int_0^{2\tau_p} B_r^{II}(\varphi, R_1)\, B_\varphi^{II}(\varphi, R_1)\, d\varphi \qquad (12)$$

B_r^{II} and B_φ^{II} correspond respectively to normal and circumferential components of magnetic flux density vector in the air-gap.

Since for the AM the magnetic flux density components in the air-gap can be directly computed using the analytical solution of magnetic scalar potential (13), the analytical formal expression of cogging torque can be obtained as given by Equation (14).

$$\vec{B} = B_r^{II}\vec{e}_r + B_\varphi^{II}\vec{e}_\varphi = -\mu_0 \cdot \vec{\nabla} U^{II} = -\mu_0 \cdot \left(\frac{\partial U^{II}}{\partial r}\vec{e}_r + \frac{1}{r}\frac{\partial U^{II}}{\partial \varphi}\vec{e}_\varphi \right) \qquad (13)$$

$$\Gamma_{cogging} = 2 \cdot l_a \cdot \mu_0 \cdot \pi \cdot \sum_{n=1}^{+\infty} (n \cdot p)^2 \cdot \left[b_{1n} \cdot b_{4n} - b_{2n} \cdot b_{3n} \right] \qquad (14)$$

For the MBGRN modeling approach the flux density components distributions in the air-gap are first computed for different positions. To do so, these components are computed for each node located at $r = R_1 + (3 \cdot e/4)$, for every position. Figure 9 illustrates how these components are estimated for a given node i. The fluxes flowing in the four branches connected to this node are first computed by following formulas

$$\begin{cases} \Phi_{1r} = \dfrac{U_{(i-m)} - U_i}{\Re_{1r}} \\[4mm] \Phi_{2r} = \dfrac{U_i - U_{(i+m)}}{\Re_{2r}} \end{cases}, \text{ for radial branches} \qquad (15)$$

$$\begin{cases} \Phi_{1\varphi} = \dfrac{U_{(i-1)} - U_i}{\Re_{1\varphi}} \\[4mm] \Phi_{2\varphi} = \dfrac{U_i - U_{(i+1)}}{\Re_{2\varphi}} \end{cases}, \text{ for circumferential branches} \qquad (16)$$

and finally, flux density components are estimated as follows

$$\begin{cases} B_r = \dfrac{1}{2} \cdot \left(\dfrac{\Phi_{1r}}{\left(\dfrac{\pi}{p \cdot m} \cdot (R_2 - h) \right) \cdot l_a} + \dfrac{\Phi_{2r}}{\left(\dfrac{\pi}{p \cdot m} \cdot R_2 \right) \cdot l_a} \right) \\[6mm] B_\varphi = \dfrac{1}{2} \cdot \left(\dfrac{\Phi_{1\varphi}}{2 \cdot h \cdot l_a} + \dfrac{\Phi_{2\varphi}}{2 \cdot h \cdot l_a} \right) \end{cases} \qquad (17)$$

where, $h = (R_4 - R_0)/82$.

The cogging torque is then computed for each position numerically using the same formula given by Equation (12) applied at $r = R_1 + (3 \cdot e / 4)$.
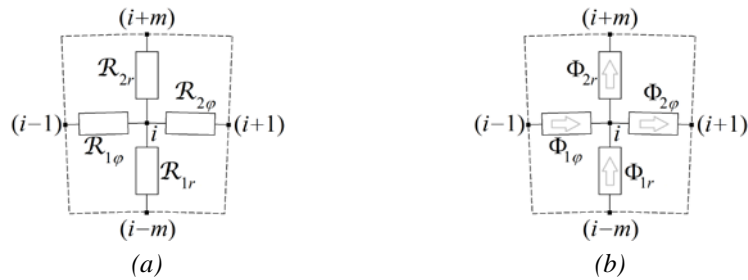

Figure 9. Computation of magnetic flux density components of node i

5.3. Computation of iron loss

The iron loss density is calculated in stator core region using the experimentally verified iron loss density model defined in (Bertotti *et al.,* 1991), (18)-(20) being, respectively, the hysteresis loss component (neglecting minor hysteresis loops), the classical eddy-current loss component, and the excess eddy-current loss component.

$$P_h = k_h f \, B_m^2 \tag{18}$$

$$P_c = \frac{\pi \sigma \, d^2 f^2}{6} \int_{2\pi} \left(\frac{dB}{d\theta_e} \right)^2 d\theta_e \tag{19}$$

$$P_e = \sqrt{2\pi} k_e f^{\frac{3}{2}} \int_{2\pi} \left| \frac{dB}{d\theta_e} \right|^{\frac{3}{2}} d\theta_e \tag{20}$$

where f and B_m are the frequency and amplitude of the fundamental flux density, θ_e is the equivalent electrical angle, σ and d are the electrical conductivity, and the lamination thickness, respectively. k_h and k_e are experimentally determined loss coefficients. These formula are applied to both flux density components separately and then summed. The flux density components in reluctance elements in stator's ferromagnetic regions are estimated using same approach explained in previous section. Exactly same approach is applied for the HAM and MBGRN models.

6. Comparison study

The open circuit performance obtained from both models are compared and results quality are assessed using results obtained from FE analyses. FE simulations are considered as a reference due to the fact that FE method is being known as giving relatively good results as compared to experimental measurements. The comparison study covers local and global quantities.

6.1. Local quantities

Figures 10-11 compare magnetic field density components spatial distribution, at $r = R_1 + (3 \cdot e/4)$, for a given value of φ_d, obtained from both methods, to corresponding results from the FE analysis. As can be seen, relatively good agreement is obtained.

While the computation time for solving the RN model is equal to 56 seconds, it is only equal to 28 seconds for the HAM. Both durations are estimated by including the elements calculation of system matrices $[P]$ and $[A]$, and sources vectors, $[\Phi]$ and $[B]$. This can correspond to both meshing and solving processes durations in FE analysis.

6.2. Global quantities

Figures 12-14 compare EMF, cogging torque waveforms and stator iron losses respectively. As can be seen, a good agreement between the three approaches is again observed. It is quite difficult to distinguish between the curves obtained from the three approaches for EMF and cogging torque waveforms.

The entire process, which includes the meshing and generation of matrix [P] and vector [Φ] elements, and the solving process, at each displacement, for the cogging computation, took 484 seconds for the RN modeling approach and 340 seconds for the HAM.
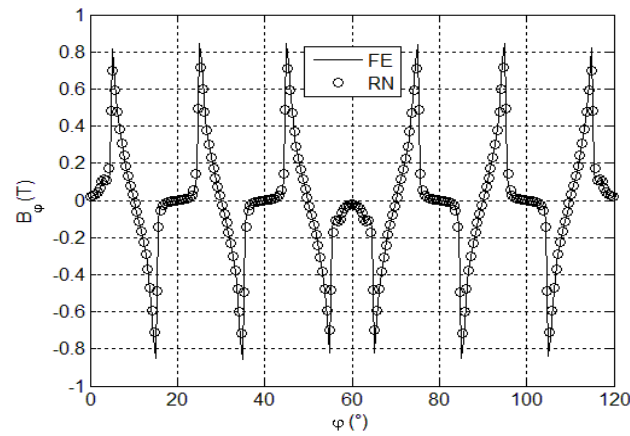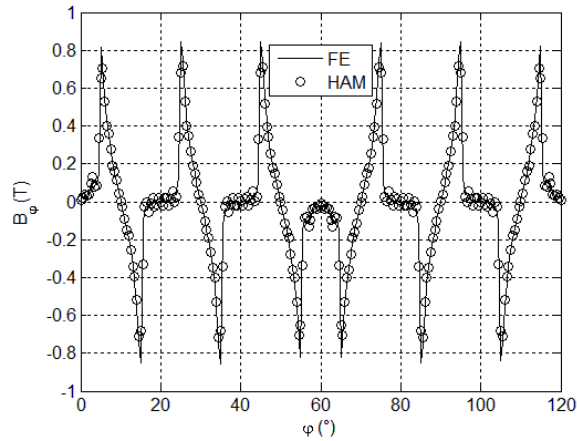

(a) Tangential component
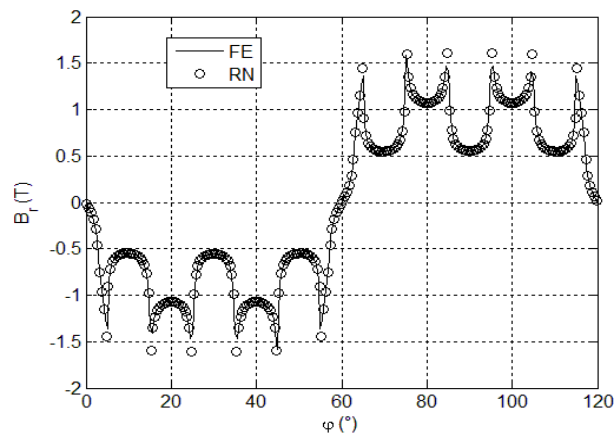
(b) Normal component

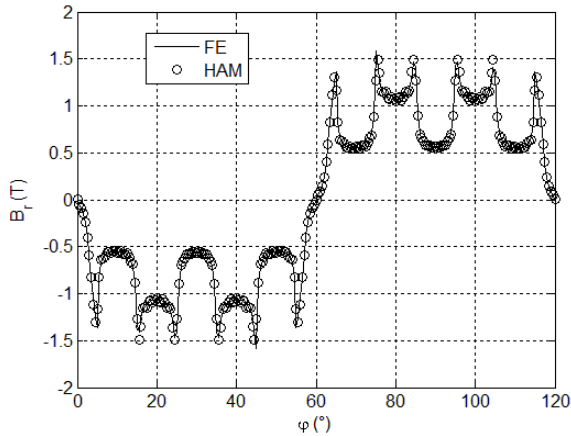*Figure 10. Comparison of RN model results with FE modeling ones*

7. Conclusion

In this paper two approaches which can be used for the pre-design of electrical structures, MBGRN and HAM, have been compared essentially in term of computation duration. It has been shown that the new HAM shows better performance, as compared to RN, for the pre-design process.

Results obtained from both methods have been compared to corresponding FE analysis, and very good agreement has been observed. This has been the case for both local and global quantities. The relative error of global quantities computed using both approaches (MBGRN and HAM) as compared to FE results is less than 5%.

(a) Tangential component

(b) Normal component

Figure 11. Comparison of HAM model results with FE modeling ones

As a perspective, the comparison will be further extended to include the mesh optimisation for both methods. This point deserves to be explored, also because it will help to further improve the computation time of these models used in the pre-design stage.
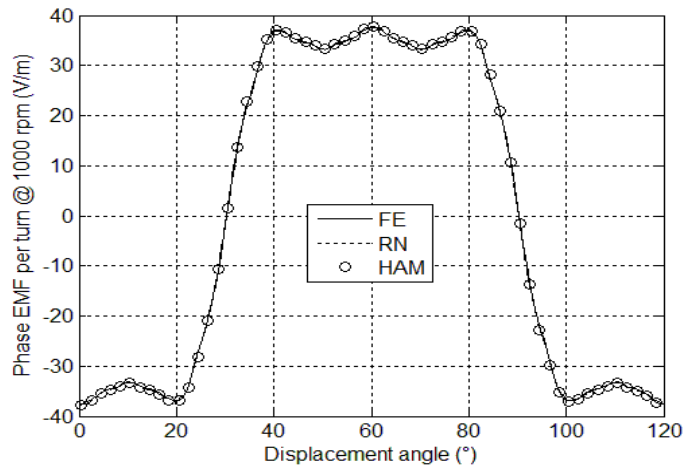

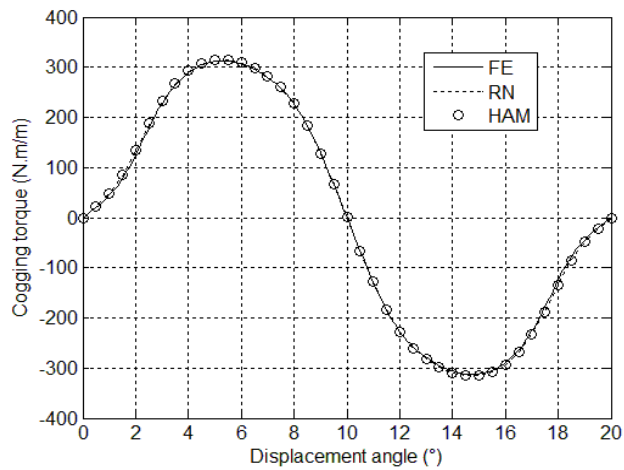*Figure 12. Comparison of EMF waveforms*

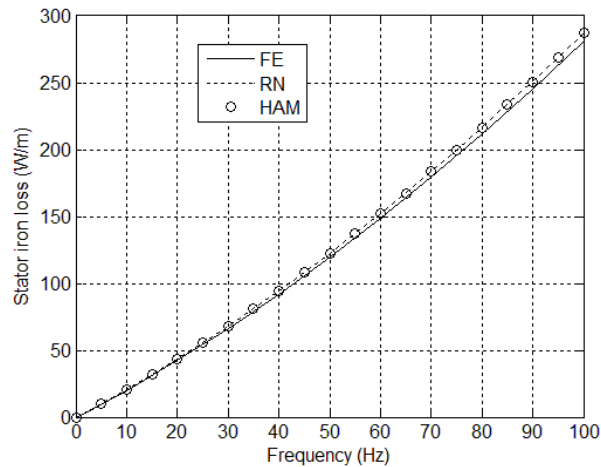*Figure 13. Comparison of cogging torque waveforms*

Figure 14. Comparison of iron losses.

Bibliography

Amara Y., Reghem P., and Barakat G. (2010). Analytical prediction of eddy-current loss in armature windings of permanent magnet brushless AC machines. *IEEE Trans. Magn.,* vol. 46, n° 8, p. 3481-3484.

Amrhein M. and Krein T. K. (2009). 3-D Magnetic equivalent circuit framework for modeling electromechanical devices. *IEEE Trans on Energy Convers,* vol. 24, n° 2, p. 397-405.

Barakat G. and Amara Y. (2014). A simple and effective way to couple analytical formal solution of magnetic potential and reluctance network models, Proceedings of 9th IET International Conference on Computation in Electromagnetics (CEM 2014), pp. 1-2, March 31 2014-April 1 2014, London.

Bellara A., Bali H., Belfkira R., Amara Y., and Barakat G. (2011). Analytical prediction of open-circuit eddy-current loss in series double excitation synchronous machines. *IEEE Trans. Magn.,* vol. 47, n° 9, p. 2261–2268.

Bertotti G., Boglietti A., Mario C, Chiampi D., Fiorillo F. and Lazzari M. (1991). An improved estimation of iron losses in electrical machines. *IEEE Trans. Magn.,* vol. 27, n° 6, p. 5007-5009.

Gholizad H., Mirsalim M. and Mirzayee M. (2006). Dynamic analysis of highly saturated switched reluctance motors using coupled magnetic equivalent circuit and the analytical

solution, in Proceedings of CEM 2006, *International Conference on Computational Electromagnetics* 2006, Aachen, Germany.

Mirzaei M., Mirsalim M., Cheng W. and Ghoizad H. (2007).   Analysis of solid rotor induction machines using coupled analytical method and reluctance networks. *International Journal of Applied Electromagnetics and Mechanic,* vol. 25, p. 193-197.

Nedjar B. (2011). *Modélisation basée sur la méthode des réseaux de perméances en vue de l'optimisation de machines synchrones à simple et à double excitation.* Thèse de Doctorat, Ecole Normale Supérieure de Cachan, Décembre 2011 (Ph. D. Thesis manuscript, in french).

Ouagued S., Amara Y. and Barakat G. (2014).   Comparison of hybrid analytical modelling and reluctance network modelling for pre-design purposes, *in Proceedings of ELECTRIMACS 2014,* Valencia, Spain.

Perho J. (2002). Reluctance network for analysing induction machines, *Acta Polytechnica Scandinavica, Electrical Engineering Series, no. 110, Espoo 2002*, Finish Academies of Technology.

Sykulski J. (1995). Computational magnetics, James & James (Science Publishers) Ltd and *Chapman & Hall*, 1995.

Tiegna H., Amara Y. and Barakat G. (2013). Overview of analytical models of permanent magnet electrical machines for analysis and design purposes. *Mathematics and Computers in Simulation,* vol. 90, p. 162-177.